PHYSICAL REVIEW B **68**, 241303(R) (2003)

Hysteretic dynamic nuclear polarization in GaAs/$Al_xGa_{1-x}As$ (110) quantum wells

H. Sanada,[1] S. Matsuzaka,[1] K. Morita,[1,2] C. Y. Hu,[1,3] Y. Ohno,[1,3,*] and H. Ohno[1,2]
[1]*Laboratory for Electronic Intelligent Systems, Research Institute of Electrical Communication, Tohoku University, Katahira 2-1-1, Aoba-ku, Sendai 980-8577, Japan*
[2]*ERATO Semiconductor Spintronics Project, Japan Science and Technology Corporation, Japan*
[3]*CREST, Japan Science and Technology Corporation, Japan*
(Received 28 August 2003; published 15 December 2003)

We investigated the dynamics of a coupled electron-nuclear spin system in a GaAs/AlGaAs (110) quantum well by time-resolved Faraday rotation measurements. Photoexcited electron spins with long coherence time ($T_2^*=6$ ns) are strongly subject to a nuclear field as well as polarizing the nuclei. A hysteretic behavior was observed in the magnetic-field dependence of the nuclear polarization under optical orientation. Our quantitative analysis based on self-consistent calculations reproduced the experimental observation of the bistable configurations of dynamic nuclear polarization.

DOI: 10.1103/PhysRevB.68.241303 PACS number(s): 78.47.+p, 78.66.Fd, 76.70.Fz

In the last decade spin-related phenomena in semiconductors have attracted considerable attention from both viewpoints of physics and applications.[1,2] Stimulated partly by proposals for applications to solid-state quantum information devices,[3,4] many efforts have been devoted to manipulate and detect local nuclear spins in semiconductor quantum structures.[5–11] Since 1960s, dynamic nuclear polarization (DNP) and related phenomena have been studied by optical methods.[12] In particular, optical time-resolved experiments have demonstrated to provide rich information about coherent spin dynamics in semiconductor quantum structures[6–8] and magnetic/nonmagnetic hybrid structures,[9] where nuclear spins play a critical role in determining their optical and/or electrical responses.

An *n*-type GaAs/AlGaAs (110) quantum well (QW) provides a favorable situation for investigation of coupled spin dynamics of electrons and nuclei. Long spin lifetime of photoexcited electrons ($\sim$several nanoseconds) and quite anisotropic *g*-tensor $\hat{g}$ can enhance DNP and, in turn, the electronic spin polarization is strongly modified by the nuclear polarization.[13] In addition, long spin coherence time allows us to obtain high-resolution energy spectra by time-resolved measurements, such as all-optical nuclear magnetic resonance (NMR).[6,13]

It has been reported that the anisotropy of $\hat{g}$ gives rise to bistability of DNP, which was first observed in GaAs/AlGaAs (100) QW's by magnetic photoluminescence (PL)-polarization measurements.[14] Compared to such conventional cw-PL polarization techniques based on the oblique Hanle effect, time-resolved Faraday rotation (TRFR) measurement is more suitable for quantitative investigation of coupled electron-nuclear spin systems. Even when a strong effective magnetic field is acting on the electron spins, for example, magnitudes and directions of both electron and nuclear spin vectors can be determined by analyzing the TRFR data. In this Rapid Communication, we investigate a bistability and a hysteretic behavior of DNP in (110) QW by TRFR method. From the magnetic field dependence of the Larmor precession frequency, we reconstruct the bistable spin configurations and explore the temporal evolution of DNP in a coupled electron-nuclear spin system.

In our experimental setup for TRFR measurements, we used a mode-locked Ti:Sapphire laser to generate $\sim$100 fs pulses at 76 MHz: the center of the photon energy spectrum was tuned at the lowest heavy hole exciton absorption peak (1.568 eV) for resonant excitation at 4.5 K. The laser pulse is divided into pump and probe beams with tunable time delay Δt: a circularly polarized pump pulse excites $\approx 10^{10}$ cm^{-2} spin-polarized electrons in a spot diameter of about 100 μm, while their time evolutions are traced by measuring Faraday rotation angles θ_F of the linearly polarized probe pulses.

The sample studied here has a 7.5-nm thick Si-doped GaAs/$Al_{0.3}Ga_{0.7}As$ QW grown on semi-insulating (110) GaAs substrate by molecular beam epitaxy. The carrier density and the Hall mobility are 1.1×10^{11} cm^{-2} and 3500 cm^2/Vs, respectively, at room temperature. The GaAs substrate was removed by a selective liftoff technique[15] and the QW was glued on quartz plate for transmission measurements. It was then placed in a magneto-optical cryostat so that the $[1\bar{1}0]$ axis in the QW plane was perpendicular to the external magnetic field $\boldsymbol{B}_{ext}$, and the [001] axis was tilted by 20° with respect to $\boldsymbol{B}_{ext}$ in order to enhance dynamic nuclear polarization.

Figure 1 shows $\theta_F(B_{ext})$ measured under right (σ^+) and left (σ^-) circular-polarizations pump at $\Delta t=1$ ns. B_{ext} was swept up and down between ±2 T at 50 mT/min. Even when a small but nonzero B_{ext} is applied, θ_F starts to oscillate rapidly with B_{ext} as a result of drastic increase of a nuclear field associated with the development of DNP. Because of the anisotropy of $\hat{g}$ and DNP, θ_F is asymmetric with respect to the origin of B_{ext}. In addition, $\theta_F(B_{ext})$ draws a hysteresis loop in positive B_{ext} with σ^- excitation and negative B_{ext} with σ^+ excitation, below 1.2 T. This hysteresis in $\theta_F(B_{ext})$ originates from the bistability of DNP.[14] Reversing the pump polarization at a fixed B_{ext} rearranges both electron and nuclear spin polarizations in a time scale of $\sim$10 sec. This is about ten times shorter than that for bulk GaAs,[5] suggesting that the hyperfine interaction is enhanced by quantum confinement of electrons with long spin relaxation time.[13] Looking into $\theta_F(B_{ext})$ after applying high B_{ext} (the sweep-down curve shown in the inset of Fig. 1), we found that $\theta_F(B_{ext})$ has two oscillating components: one with long

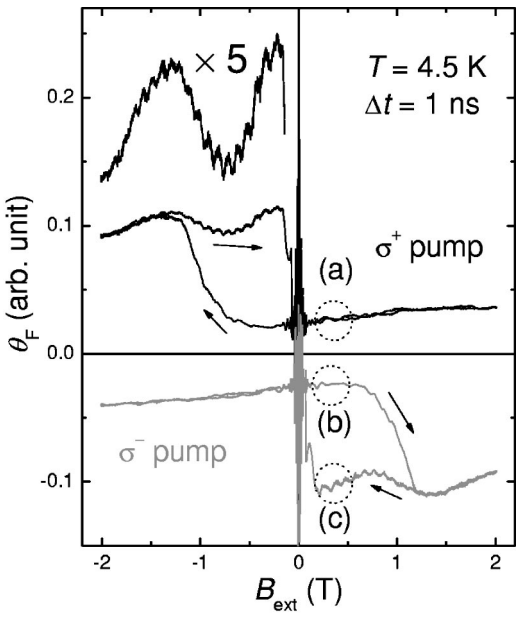

FIG. 1. External magnetic field B_{ext} dependence of Faraday rotation θ_F at a fixed delay time $\Delta t = 1$ ns is shown by black (σ^+ pump) and gray (σ^- pump) lines, respectively. The measurements were done at 4.5 K with the sample tilted by 20° off from $\boldsymbol{B}_{ext}$. The sweep rate of B_{ext} was 50 mT/min. Time-resolved θ_F at $B_{ext} = 0.3$ T for three different conditions, labeled by (a), (b), and (c), are shown in Fig. 2. Inset: Expanded data when B_{ext} was swept from -2 T to 0 T under σ^+ pump.

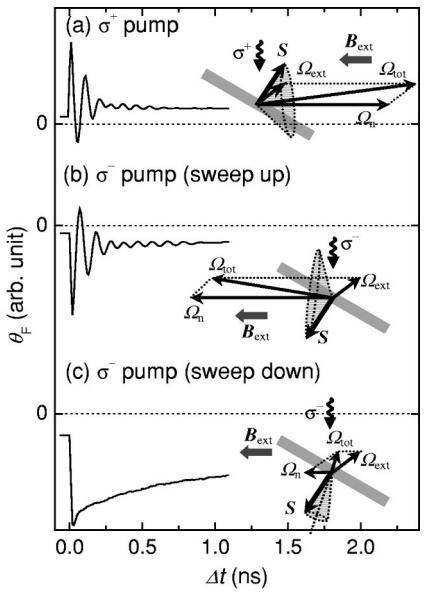

FIG. 2. (a) Time-resolved Faraday rotation angle $\theta_F(\Delta t)$ measured at 4.5 K and 0.3 T under σ^+ pump. (b) $\theta_F(\Delta t)$ measured at 0.3 T under σ^- pump when B_{ext} was swept up and (c) when B_{ext} was swept down, respectively. The insets show each configuration of the vectors of nuclear field ($\boldsymbol{\Omega}_n$), external field ($\boldsymbol{\Omega}_{ext}$), and the total field ($\boldsymbol{\Omega}_{tot}$) in the unit of frequency.

period which represents a change in phase owing to variation of B_{ext} and the other with much shorter period seen only when $B_{ext} < 1$ T comes from the interference with the past-injected electron spins, which appears when the effective spin coherence time T_2^* is comparable or longer than the pulse interval.[16,17] By fitting the waveform of $\theta_F(B_{ext})$, we obtained T_2^* of 6 ns.

Next we investigated the hysteretic DNP by analyzing θ_F measured in the time domain. In Figs. 2(a)–2(c) are plotted $\theta_F(\Delta t)$ measured at $B_{ext} = 0.3$ T for three cases labeled by (a), (b), and (c) in Fig. 1, respectively. In general, $\theta_F(\Delta t)$ consists of a sum of two components: $C_1 \exp(-\Delta t/T_1) + C_2 \exp(-\Delta t/T_2^*)\cos(|\boldsymbol{\Omega}_n + \boldsymbol{\Omega}_{ext}|\Delta t)$, where C_1 and C_2 are constants, and an external magnetic field $\boldsymbol{\Omega}_{ext}$ and a nuclear field $\boldsymbol{\Omega}_n$ are expressed in the unit of frequency.[13] The first term represents the longitudinal spin component with spin relaxation time T_1, while the latter is transverse spin component oscillating at Larmor frequency $\Omega_{tot} = |\boldsymbol{\Omega}_n + \boldsymbol{\Omega}_{ext}|$ with T_2^*. Under σ^+-pump, $\theta_F(\Delta t)$ oscillates at high frequency with $C_2 > C_1$, as shown in Fig. 2(a). The inset illustrates the configuration of the effective fields reconstructed from the data. Although $\boldsymbol{\Omega}_{ext} = (\mu_B/\hbar)\hat{g}\boldsymbol{B}_{ext}$ is small and turns away from $\boldsymbol{B}_{ext}$, where μ_B is the Bohr magneton and $\hbar$ is the reduced Plank constant, the total effective field $\boldsymbol{\Omega}_{tot} = \boldsymbol{\Omega}_{ext} + \boldsymbol{\Omega}_n$ is large and nearly parallel to the QW so that the tip of electron spin $\boldsymbol{S}$ should draw a large circle perpendicular to the QW plane.

For σ^- pump, we obtained two different results as shown in Figs. 2(b) and 2(c). When B_{ext} is swept up from 0 to 0.3 T [Fig. 2(b)], the features of $\theta_F(\Delta t)$ are almost the same as that of σ^+ pump (a) except for the sign. When B_{ext} was swept down from 2 to 0.3 T [Fig. 2(c)], on the other hand, the oscillating component almost disappeared: this suggests that $\boldsymbol{\Omega}_{tot}$ is almost perpendicular to the QW plane as shown in Fig. 2(c).

It should be noted that $\theta_F(\Delta t)$ in Figs. 2(a) and 2(b) cannot be fitted completely with the above expression: there exists some "beat" on its oscillating part, but it is too small to distinguish two or more Ω_{tot} by Fourier analysis of the experimental results. Together with this, the fact that T_2^* decreases significantly with applying B_{ext} suggests an inhomogeneity in $\boldsymbol{\Omega}_n$ and/or $\hat{g}$ within the laser spot in the present sample.[13]

For quantitative discussion, we calculated average electron spin $\langle \boldsymbol{S} \rangle$ and nuclear spin $\langle \boldsymbol{I} \rangle$ to reproduce the experimental results. The expression of $\langle \boldsymbol{S} \rangle$ is given by

$$\langle \boldsymbol{S} \rangle = \frac{c\boldsymbol{S} \cdot \boldsymbol{\Omega}_{tot}}{|\boldsymbol{\Omega}_{tot}|^2} \boldsymbol{\Omega}_{tot}, \tag{1}$$

where c represents the reduction of electron spin due to imperfect selective excitation and spin relaxation. Provided that $\langle \boldsymbol{I} \rangle$ is proportional to $\langle \boldsymbol{S} \rangle \cdot \boldsymbol{B}_{ext}$, nuclear field can be expressed as[18]

$$\boldsymbol{\Omega}_n = \frac{4}{3}\frac{A}{\hbar} I(I+1) \frac{\langle \boldsymbol{S} \rangle \cdot \boldsymbol{B}_{ext}}{|\boldsymbol{B}_{ext}|^2 + B_{loc}^2} \boldsymbol{B}_{ext} f, \tag{2}$$

where A is a hyperfine constant, $I = 3/2$ for Ga and As nuclei, and f a leakage factor. B_{loc} is an effective fluctuating field, which acts on local nuclei and generally refers to dipole-

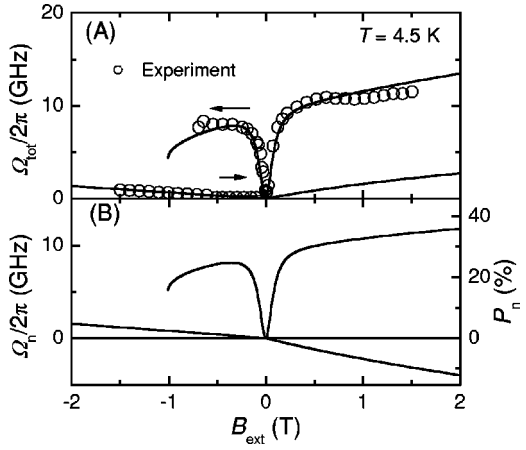

FIG. 3. Calculated Ω_{tot} (*A*) and Ω_n (*B*) are plotted by solid lines. Experimental values of Ω_{tot} at 4.5 K are plotted in (*A*) by circles.

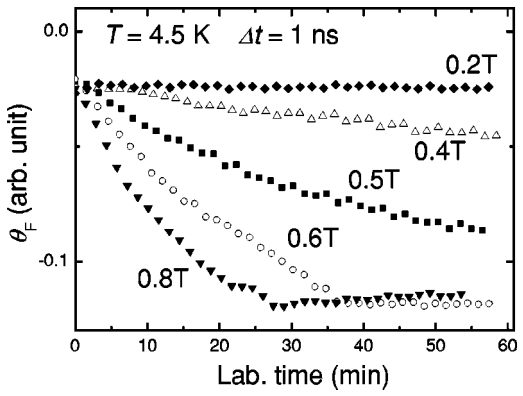

FIG. 4. Laboratory time dependence of θ_F with $B_{ext}=0.2,0.4,0.5,0.6$, and 0.8 T under σ^- pump. The temperature was 4.5 K and Δt was fixed at 1 ns. The data were recorded after B_{ext} was swept from 0 T to a predetermined B_{ext} at 154 mT/min.

dipole interaction between neighboring nuclei.[18] $\mathbf{\Omega}_n$, given by Eq. (2), then modifies $\langle \boldsymbol{S} \rangle$ according to $\mathbf{\Omega}_{tot}=\mathbf{\Omega}_{ext}+\mathbf{\Omega}_n$. To obtain $\mathbf{\Omega}_{tot}$ and $\mathbf{\Omega}_n$ we solved Eqs. (1) and (2) self-consistently. In the calculation, the effective g factors $g[001]=-0.04$ and $g[110]=-0.19$ determined experimentally by reducing the pump power to suppress possible nuclear effect were used. We took $(A/\hbar)cf$ $[=68.5\times10^9$ (rad/s)] as a fitting parameter. Taking $B_{loc}=0.1$ mT,[18] the calculated Ω_{tot} considerably deviates from the experimental data when $|B_{ext}|<0.3$ T (not shown). Instead, we calculate Ω_{tot} by taking B_{loc} as a fitting parameter and obtained the best fit with $B_{loc}=80$ mT, as shown by the solid lines in Fig. 3(a). This value of B_{loc} is much greater than the known dipole-dipole interaction between neighboring nuclei, but consistent with those reported in other recent studies in which a nuclear field disappears around $B_{ext}=10\sim100$ mT.[9,19]

By solving Eqs. (1) and (2), two sets of solutions $\Omega_{tot}^{\pm}$ and $\Omega_n^{\pm}$ are obtained for $B_{ext}>-1.01$ T: As $B_{ext}<0$ T, Ω_{tot}^{+} and Ω_{tot}^{-} agree well with the experimental data shown in Figs. 2(b) and 2(c), respectively. When $B_{ext}>0$, there also exist two possible $\Omega_{tot}^{\pm}$ but only Ω_{tot}^{+} was observed in the experiment [Fig. 2(a)].[20] In Fig. 3(b) the degree of the nuclear spin polarization $P_n \propto \Omega_n$ is also shown on the right axis, assuming that the maximum Ω_n is 205.5×10^9 rad/s with all the nuclei fully polarized.[18] It is found that the maximum P_n reaches over 30% at $B_{ext}=1.5$ T.

Finally we examined the temporal evolution of DNP toward stable configuration by monitoring θ_F in laboratory time t. Under σ^- pump, B_{ext} was swept up quickly (154 mT/min) from 0 T and stopped at a certain magnetic field, at which the spin system has not reached the steady state. Then $\theta_F(t)$ (at $\Delta t=1$ ns) was measured with B_{ext} fixed. For several B_{ext} we plot the results in Fig. 4. As $B_{ext}\geqslant0.4$ T, $\theta_F(t)$ approaches gradually toward the stable configuration in a few tens of minutes. When $B_{ext}=0.2$ T, the system remains in the initial configuration at least for an hour. From these results, critical fields for transitions between $\Omega_{tot}^{\pm}$ configurations are difficult to define. We also measured $\theta_F(\Delta t)$ within the duration of these transitions (not shown). The features of such $\theta_F(\Delta t)$ are complex and cannot be explained by simply assuming a single configuration of $\langle \boldsymbol{I} \rangle$ and $\boldsymbol{S}$ rather they appear as a mixture of the two or more configurations. This suggests formation of domains of coupled electron-nuclear spin system, i.e., the transition between bistable configurations appears to take place locally in wide-spread time scales.

In conclusion, we investigated the dynamics of a coupled electron and nuclear spin system in *n*-GaAs/AlGaAs (110) QW by TRFR measurements. Bistability of dynamic nuclear polarization is observed under optical orientation. The experimental results are reproduced quite well by the self-consistent calculation, in which the best fit was obtained when a local fluctuating field for nuclei is assumed to be 80 mT, much larger than the neighboring dipole-dipole interaction. This bistability might be applied to effective control of nuclear polarization via small external field or gate control via modulation of the effective g factors.[21]

The authors wish to acknowledge F. Matsukura, K. Ohtani, and M. Kohda for useful discussion. This work was partly supported by the Ministry of Education, Culture, Sports, Science and Technology (MEXT), Japan Society for the Promotion of Science (JSPS), and the 21st Century COE program ''System Construction of Global-Network Oriented Information Electronics,'' at Tohoku University.

*Electronic address: oono@riec.tohoku.ac.jp

[1] H. Ohno, F. Matsukura, and Y. Ohno, *JSAP International* (Japan Society of Applied Physics, Tokyo, 2002), Vol. 5, pp. 4–13, available at http://www.jsapi.jsap.or.jp/

[2] *Semiconductor Spintronics and Quantum Computation*, edited by D.D. Awschalom, N. Samarth, and D. Loss (Springer-Verlag, Berlin, 2002).

[3] B.E. Kane, Nature (London) **393**, 133 (1998).

[4] T.D. Ladd, J.R. Goldman, F. Yamaguchi, Y. Yamamoto, E. Abe, and K.M. Itoh, Phys. Rev. Lett. **89**, 017901 (2002).

[5] J.M. Kikkawa and D.D. Awschalom, Science **287**, 473 (2000).

[6] G. Salis, D.T. Fuchs, J.M. Kikkawa, D.D. Awschalom, Y. Ohno,

and H. Ohno, Phys. Rev. Lett. **86**, 2677 (2001).

[7] A. Malinowski and R.T. Harley, Solid State Commun. **144**, 419 (2000).

[8] D. Gammon, S.W. Brown, E.S. Snow, T.A. Kennedy, D.S. Katzer, and D. Park, Science **277**, 85 (1997).

[9] R.K. Kawakami, Y. Kato, M. Hanson, I. Malajovich, J.M. Stephens, E. Johnston-Halperin, G. Salis, A.C. Gossard, and D.D. Awschalom, Science **294**, 131 (2001).

[10] K. Ono and S. Tarucha (unpublished).

[11] T. Machida, T. Yamazaki, K. Ikushima, and S. Komiyama, Appl. Phys. Lett. **82**, 409 (2003).

[12] *Optical Orientation*, edited by F. Meier and B.P. Zakarchenya (Elsevier, Amsterdam, 1984).

[13] G. Salis, D.D. Awschalom, Y. Ohno, and H. Ohno, Phys. Rev. B **64**, 195304 (2001).

[14] V.K. Kalevich and V.L. Korenev, Pisfma Zh. Eks. Teor. Fiz. **56**, 257 (1992) [JETP Lett. **56**, 253 (1992)].

[15] E. Yablonovitch, T. Gmitter, J.P. Harbison, and R. Bhat, Appl. Phys. Lett. **51**, 2222 (1987).

[16] J.M. Kikkawa and D.D. Awschalom, Phys. Rev. Lett. **80**, 4313 (1998).

[17] Although all-optical NMR at the optical chopper frequency is another possible mechanism for the origin of an oscillation in low B_{ext} (Ref. 6), it is not the case here, since the oscillatory features did not depend on the chopper frequency.

[18] D. Paget, G. Lampel, B. Sapoval, and V.I. Safarov, Phys. Rev. B **15**, 5780 (1977).

[19] D. Gammon, Al.L. Efros, T.A. Kennedy, M. Rosen, D.S. Katzer, D. Park, S.W. Brown, V.L. Korenev, and I.A. Merkulov, Phys. Rev. Lett. **86**, 5176 (2001).

[20] In the Ω_{tot}^{-} configuration, the sign of Ω_n is negative [see Fig. 3(b)], i.e., nuclear spins must be polarized in the direction opposite to that of initially pumped electron spins. Under a fixed pump polarization, such a configuration may not be accessible.

[21] G. Salis, Y. Kato, K. Ensslin, D.C. Driscoll, A.C. Gossard, and D.D. Awschalom, Nature (London) **414**, 619 (2001); Y. Kato, R.C. Myers, D.C. Driscoll, A.C. Gossard, J. Levy, and D.D. Awschalom, Science **299**, 1201 (2003).